MDPI

Article

Stability of Periodic, Traveling-Wave Solutions to the Capillary-Whitham Equation

John D. Carter [1,*,†] and Morgan Rozman [2,†]

[1] Seattle University; carterj1@seattleu.edu
[2] Seattle University; rozmanm@seattleu.edu
* Correspondence: carterj1@seattleu.edu; Tel.: +1-206-296-5956
† These authors contributed equally to this work.

Version March 12, 2019 submitted to Fluids

Abstract: Recently, the Whitham and capillary-Whitham equations were shown to accurately model the evolution of surface waves on shallow water [1,2]. In order to gain a deeper understanding of these equations, we compute periodic, traveling-wave solutions to both and study their stability. We present plots of a representative sampling of solutions for a range of wavelengths, wave speeds, wave heights, and surface tension values. Finally, we discuss the role these parameters play in the stability of these solutions.

Keywords: Whitham equation; fully-dispersive; surface tension; traveling-wave solutions; stability

1. Introduction

The dimensionless Korteweg-deVries equation (KdV) including surface tension,

$$u_t + u_x + \left(\frac{1}{6} - \frac{T}{2}\right)u_{xxx} + 2uu_x = 0, \tag{1}$$

is an asymptotic approximation to the surface water-wave problem including surface tension in the small-amplitude, long-wavelength limit. The variable $u = u(x,t)$ represents dimensionless surface displacement, t represents the dimensionless temporal variable, x represents the dimensionless spatial variable, and $T \geq 0$ represents the dimensionless coefficient of surface tension (the inverse of the Bond number). This equation only accurately reproduces the unidirectional, linear phase velocity of the full water wave problem for a small range of wavenumbers near zero. In order to address this issue, Whitham [3,4] proposed a generalization of KdV that is now known as the Whitham equation for water waves. In dimensionless form, this equation is given by

$$u_t + \mathcal{K}u_x + 2uu_x = 0, \tag{2}$$

where $\mathcal{K}$ is the Fourier multiplier defined by the symbol

$$\widehat{\mathcal{K}f}(k) = \sqrt{(1 + Tk^2)\frac{\tanh(k)}{k}}\,\hat{f}(k). \tag{3}$$

We refer to equation (2) with $T = 0$ as the Whitham equation and (2) with $T > 0$ as the capillary-Whitham, or cW, equation. Equation (2) reproduces the unidirectional phase velocity of the water wave problem with $T \geq 0$ for all k.

In summarizing the recent work on these equations, we focus on the results that are most directly related to what we present below. Ehrnström & Kalisch [5] proved the existence of and computed periodic, traveling-wave solutions to the Whitham equation. Ehrnström *et al.* [6] proved the existence of solitary-wave solutions to the Whitham equation and showed that they are conditionally energetically stable. Arnesen [7] proved the existence of solitary-wave solutions to the capillary-Whitham equation and showed that they are conditionally energetically stable. Johnson & Hur [8] proved that all small-amplitude, periodic, traveling-wave solutions of the Whitham equation are stable if their wavelength is above a critical value and are unstable below the critical value. Sanford *et al.* [9] numerically corroborated the Johnson & Hur [8] result and numerically established that all large-amplitude, periodic, traveling-wave solutions of the Whitham equation are unstable regardless of wavelength. Kalisch *et al.* [10] present numerical results which suggest that large-amplitude solutions of the Whitham equation are unstable. Moldabayev *et al.* [11] presented a scaling regime in which the Whitham equation can be derived from the water wave problem and compared its dynamics with those from other models including the Euler equations. Klein *et al.* [12] proved that the Whitham equation is a rigorous model of water waves in the KdV regime. The validity of the Whitham equation outside the KdV regime remains an open question. Deconinck & Trichtchenko [13] proved that the unidirectional nature of the Whitham equation causes it to miss some of the instabilities of the Euler equations. Dinvay *et al.* [14] extended the work of Moldabayev *et al.* [11] to include surface tension and show that the capillary-Whitham equation gives a more accurate reproduction of the free-surface problem than the KdV and Kawahara (fifth-order KdV) equations. Trillo *et al.* [1] compared Whitham predictions with measurements from laboratory experiments and showed that the Whitham equation provides an accurate model for the evolution of initial waves of depression, especially when nonlinearity plays a significant role. Additionally, Carter [2] compared predictions with another set of laboratory measurements and showed that both the Whitham and capillary-Whitham equations more accurately model the evolution of long waves of depression than do the KdV and Serre (Green-Naghdi) equations.

Much work has been done on equations related to the capillary-Whitham equation. Vanden-Broeck [15] provides a detailed review of gravity-capillary free surface flows. In the absence of gravity, Crapper [16] found a family of exact solutions to the water wave problem with surface tension. Trulsen *et al.* [17] presented an equation for weakly nonlinear waves on deep water with exact linear dispersion including gravity, but not surface tension. This equation is to the NLS equation, see for example Sulem & Sulem [18], as the Whitham equation is to the KdV equation. Akers *et al.* [19] prove the existence of gravity-capillary waves that are nearby to Crapper waves when the gravity effect is small. They showed numerically that these solutions are waves of depression and that there exists a wave of highest amplitude. Akers & Milewski [20,21] derive and study solitary-wave solutions of multiple full-dispersion models of gravity-capillary waves. The papers [17,20,21] all approach capillary-gravity problem from the deep-water viewpoint as opposed to the capillary-Whitham equation which comes from the shallow-water viewpoint.

Finally, the recent work by Ehrnström *et al.* [22] includes many theoretical results on solutions to the capillary-Whitham equation. It gives a complete description of all small-amplitude, periodic, traveling-wave solutions to the capillary-Whitham equation and then extends these small-amplitude results to global curves. Further, they analytically describe some secondary bifurcations that connect different branches. These results tie in nicely with the numerical results we present below.

The remainder of the paper is outlined as follows. Section 2 describes the solutions we examine, their properties, and the linear stability calculations. Section 3 contains plots of solutions to the Whitham and capillary-Whitham equations, plots of the corresponding stability spectra, and a discussion of these results. Section 3 contains the main results of the paper. Section 4 concludes the paper by summarizing the results.

2. Traveling waves and their stability

We consider periodic, traveling-wave solutions of the form

$$u(x,t) = f(x-ct), \tag{4}$$

where f is a smooth, periodic function with period L and c is the speed of the solution. Ehrnström & Kalisch [5] proved that the Whitham equation admits solutions of this form and Remonato & Kalisch [23] computed a variety of cW solutions of this form. Substituting (4) into (2) and integrating once gives

$$-cf + \mathcal{K}f + f^2 = B, \tag{5}$$

where B is the constant of integration. This equation is invariant under the transformation

$$f \to f + \gamma, \quad c \to c + 2\gamma, \quad B \to B + \gamma(1 - c - \gamma). \tag{6}$$

Therefore, we consider the entire family of solutions of the form given in equation (4) by considering only solutions with zero mean, that is solutions such that

$$\int_0^L f(z)\, dz = 0. \tag{7}$$

In order to study the stability of these solutions, change variables to a moving coordinate frame by introducing the coordinates, $z = x - ct$ and $\tau = t$. In the moving coordinate frame, the cW equation is given by

$$u_\tau - cu_z + \mathcal{K}u_z + 2uu_z = 0. \tag{8}$$

We consider perturbed solutions of the form

$$u_{\text{pert}}(z,\tau) = f(z) + \epsilon w(z,\tau) + \mathcal{O}(\epsilon^2), \tag{9}$$

where $f(z)$ is a zero-mean, periodic, traveling-wave solution of the cW equation (i.e. a stationary solution of (8)), $w(z,\tau)$ is a real-valued function, and ϵ is a small, positive constant. Substituting (9) into (8) and linearizing gives

$$w_\tau - cw_z + \mathcal{K}w_z + 2fw_z + 2f_z w = 0. \tag{10}$$

Without loss of generality, assume

$$w(z,\tau) = W(z)e^{\lambda\tau} + c.c., \tag{11}$$

where $W(z)$ is a complex-valued function, λ is a complex constant, and $c.c.$ denotes complex conjugate. Substituting (11) into (10) and simplifying gives

$$(c - 2f)W' - 2f'W - \mathcal{K}W' = \lambda W, \tag{12}$$

where prime means derivative with respect to z. In operator form, equation (12) can be written as

$$\mathcal{L}W = \lambda W, \quad \text{where} \quad \mathcal{L} = (c-2f)\partial_z - 2f' - \mathcal{K}\partial_z. \tag{13}$$

We are interested in finding the set of λ that lead to bounded solutions of (13). In other words, we are interested in finding the spectrum, σ, of the operator $\mathcal{L}$. The spectrum determines the spectral stability of the solutions. If $\sigma(\mathcal{L})$ has no elements with positive real part, then the solution is said to be spectrally stable. If $\sigma(\mathcal{L})$ has one or more elements with positive real part, then the solution is said to be unstable. Since the capillary-Whitham equation is Hamiltonian, see Hur & Pandey [24], $\sigma(\mathcal{L})$ is symmetric under

reflections across both the real and imaginary axes. We use this fact as one check on the numerical stability results in the next section.

3. Numerical results

In this section, we present plots of periodic, traveling-wave solutions of the Whitham and capillary-Whitham equations along with their stability spectra. The solutions were computed using a generalization of the Newton-based method presented by Ehrnström & Kalisch [5]. Following the work of Sanford *et al.* [9], the stability of these solutions was computed using the Fourier-Floquet-Hill method of Deconinck & Kutz [25].

3.1. The Whitham equation

In order to best understand the role surface tension plays in the stability of periodic, traveling-wave solutions to the capillary-Whitham equation, we begin by reviewing results from the Whitham equation (i.e. the zero surface tension case). Hur & Johnson [8] proved that all small-amplitude Whitham solutions with $k < 1.145$ (where k is the wavenumber of the solution) are stable while all small-amplitude solutions with $k > 1.145$ are unstable. Sanford *et al.* [9] numerically corroborated this result, presented numerical results that suggest that all large-amplitude Whitham solutions are unstable, and established that 2π-periodic, traveling-wave solutions with "small" wave heights are spectrally stable while those with "large" wave heights are unstable.

Figure 1 contains plots of four 2π-periodic solutions to the Whitham equation with moderate wave heights. As the wave height, H, of the solution increases, so does the solution's wave speed, c. Figure 2 contains plots of the stability spectra corresponding to these solutions. The spectrum of the solution in Figure 1(a), see Figure 2(a), lies entirely on the imaginary axis and therefore this solution is spectrally stable. Further simulations (not included) show that all solutions with smaller wave heights (and period 2π) are also spectrally stable. The spectra corresponding to the other three solutions all include eigenvalues with positive real parts and therefore these solutions are unstable. As the wave height of the solution increases, the maximum instability growth rate (i.e. the real part of the eigenvalue with maximal real part) also increases. All of these spectra include the "figure 8" associated with the modulational (Benjamin-Feir) instability.

Whitham [4] conjectured that the Whitham equation admits a highest traveling-wave solution and that it is nonsmooth. Ehrnström and Wahlén [26] proved this hypothesis. Figure 3 includes plots of six solutions that are somewhat near this highest wave. The inset plots are zooms of the solutions near their crests and show that all of the solutions we consider are smooth. To our knowledge, this is the first time that the spectral stability of solutions of the Whitham equation with wave heights this large have been studied.

Figure 4 includes the stability spectra corresponding to the solutions in Figure 3. All six of these solutions are unstable. As wave height (or wave speed) increases, the maximal instability growth rate also increases. The stability spectra undergo two bifurcations as the wave height increases. The first bifurcation is shown in Figure 4(a) and the second is shown in Figure 4(b). The first occurs when the top part of the figure 8 bends down and touches the bottom part on the $\mathcal{R}(\lambda)$ axis at around $\lambda = \pm 0.05$. (See the transition from the spectrum in Figure 2(d) to the blue spectrum in Figure 4(a).) This causes the vertical figure 8 to transition into a horizontal figure 8 inside of a vertical "peanut". (See the orange spectrum in Figure 4(a).) The second bifurcation occurs when the horizontal figure 8 collapses toward the origin and the peanut pinches off into two ovals centered on the $\mathcal{R}(\lambda)$ axis. (See Figure 4(b).) Note that the two yellow "dots" near $\lambda = \pm 0.32$ are actually small ovals. As wave height increases even further, these ovals decrease in diameter and move further away from the $\mathcal{I}(\lambda)$ axis. The solution with maximal wave height is cusped and therefore a very large number of Fourier modes would be required to resolve it accurately.

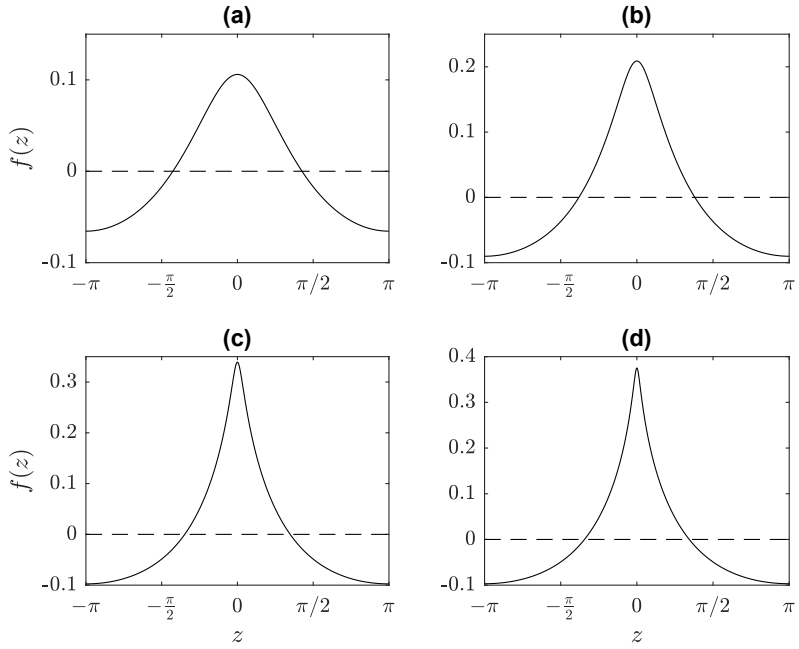

Figure 1. Plots of four moderate wave height, 2π-periodic, zero-mean solutions of the Whitham equation. The wave speeds and wave heights of these solutions are (a) $c = 0.89236$, $H = 0.17148$, (b) $c = 0.92685$, $H = 0.29901$, (c) $c = 0.96612$, $H = 0.43667$, and (d) $c = 0.97249$, $H = 0.47203$. Note that the vertical scale is different in each of the plots.

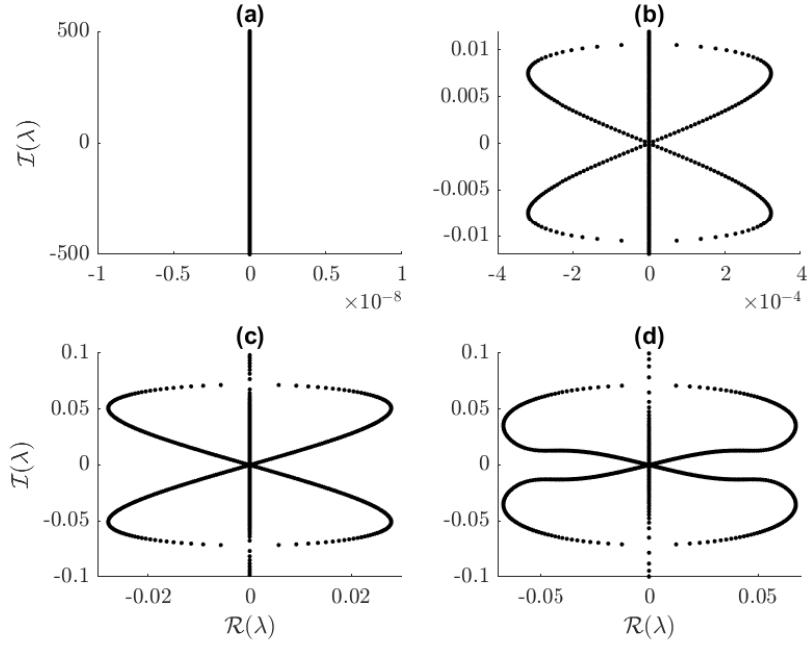

Figure 2. Spectra of the solutions shown in Figure 1. Note that both the horizontal and vertical scales vary from plot to plot.

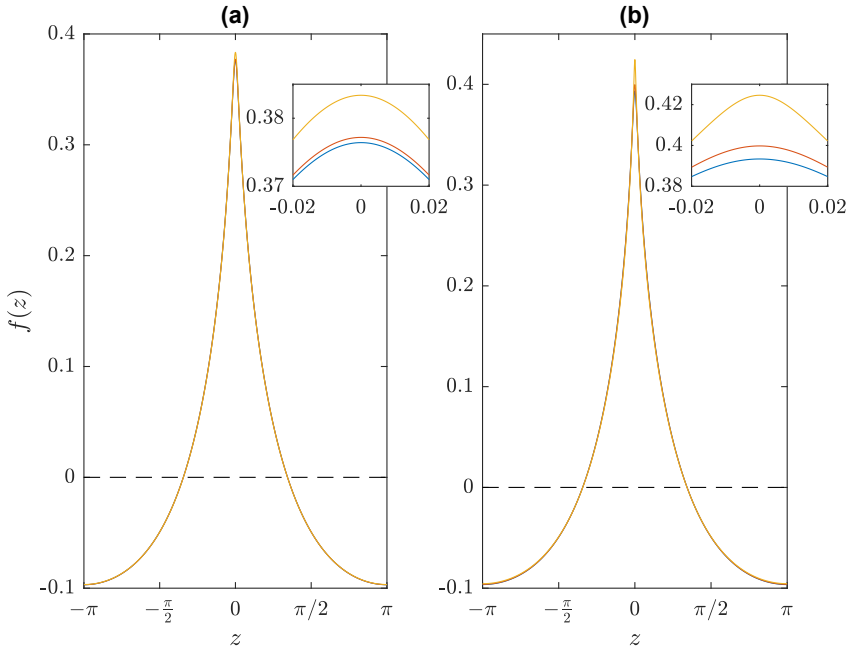

Figure 3. Figures (a) and (b) each contain three plots of large wave height, 2π-periodic, zero-mean solutions of the Whitham equation. The solutions are very similar and nearly lie on top of one another. The inset plots are zooms of the intervals surrounding the crests of the solutions. The wave speeds and heights of these solutions, in order of increasing speed, are (a) $c = 0.97266$ and $H = 0.47330$ (blue); $c = 0.97276$ and $H = 0.47405$ (orange); and $c = 0.97351$ and $H = 0.48007$ (yellow); and (b) $c = 0.97451$ and $H = 0.50058$ (blue); $c = 0.97501$ and $H = 0.499599$ (orange); and $c = 0.97596$ and $H = 0.52013$ (yellow).

This makes computing solutions near the solution with maximal wave height prohibitively expensive. The stability calculation is even more computationally expensive. Because of this, exactly what happens to the stability spectra as the wave height approaches the maximal wave height remains an open question

3.2. The capillary-Whitham equation

In this subsection, we study periodic, traveling-wave, zero-mean solutions of the cW equation and their stability. Due to the massive number of solutions this equation admits, this study is not meant to be exhaustive. We present plots of solutions and their stability spectra and end with a discussion that summarizes our observations. Ehrnström *et al.* [22] prove that small-amplitude solutions to the capillary-Whitham equation exist for all values of $T > 0$. Note that the solutions presented herein cannot be directly compared with those of Remonato & Kalisch [23] because we required the solutions to have zero mean while they did not. However, the two sets of solutions are related via the transformation given in equation (6).

We begin by justifying the values we selected for the capillarity/surface tension parameter, T. The Fourier multiplier $\mathcal{K}$ undergoes a bifurcation at $T = \frac{1}{3}$. When T=0, $\mathcal{K}$ decreases monotonically to zero as the wavenumber of the solution, $k > 0$, increases. When $T \in (0, \frac{1}{3})$, $\mathcal{K}$ achieves a unique local minimum at some wavenumber $k^* \in (0, \infty)$. When $T > \frac{1}{3}$, $\mathcal{K}$ increases monotonically for all $k > 0$ and therefore $\mathcal{K}$ has is no local minimum. Because of this behavior, we selected $T = 0.2$, $\frac{1}{3}$, and 0.4. Additionally, we study solutions for $T \approx 0.1582$ (see Section 3.2.4 for details). Figure 5 contains plots of $\mathcal{K}$ versus k for each of these T values and demonstrates the bifurcation.

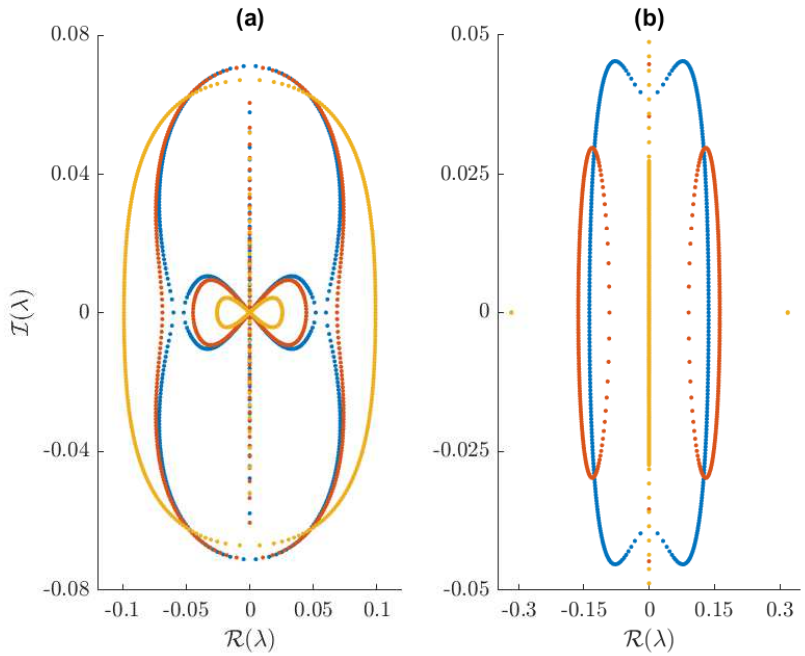

Figure 4. Spectra of the solutions shown in Figure 3.

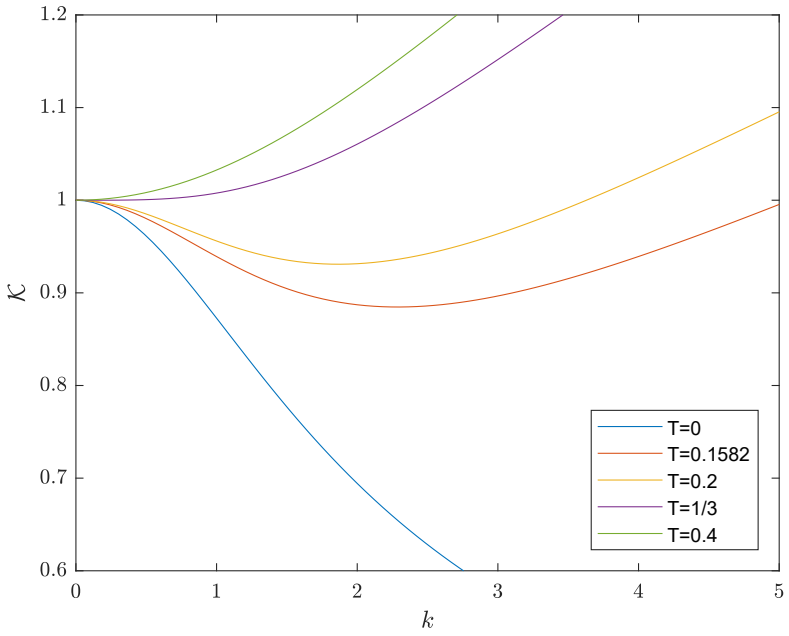

Figure 5. Plots of $\mathcal{K}$ versus k for each of the five values of T examined herein.

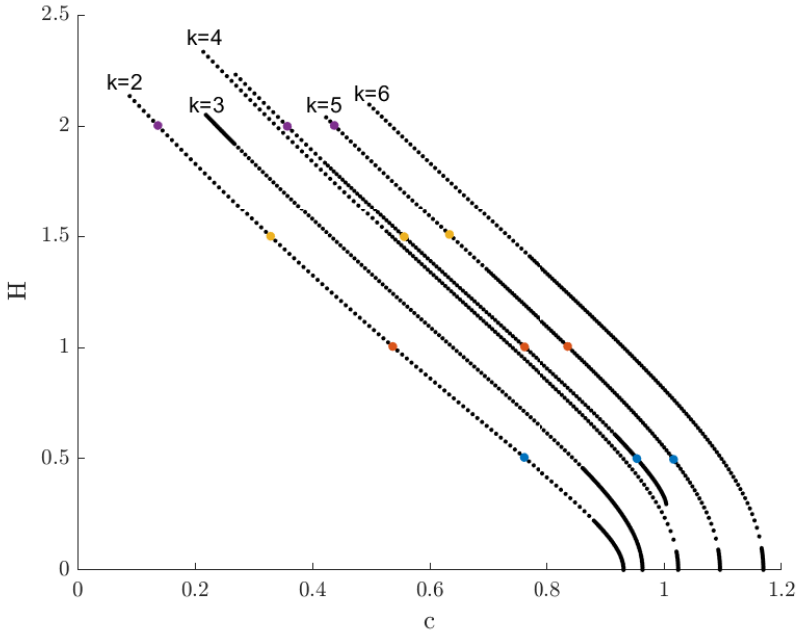

Figure 6. A portion of the wave height versus wave speed bifurcation diagram for the cW equation with $T = 0.2$. The colored dots correspond to solutions that are examined in more detail in Figures 7-9.

3.2.1. Surface tension parameter $T = 0.2$

When $T = 0.2$, we were able to compute solutions with wavenumbers greater than $k \approx 1.9$, but were not able to compute solutions with wavenumber less than $k \approx 1.9$. (Note that we computed solutions with both integer and non-integer wavenumbers.) This may be related to Proposition 5.2 of Ehrnström *et al.* [22] which states that there are regions of (k, T)-space where no periodic solutions of the capillary-Whitham equation exist. This may also be related to the fact that $k^* \approx 1.9$. (Recall that k^* is the location of the local minimum of $\mathcal{K}$ when $T < \frac{1}{3}$.) Figure 6 includes a portion of the wave height versus wave speed bifurcation diagram for this case. It includes the bifurcation branches corresponding to the $k = 2, \ldots, 6$ solutions as well as an additional branch that splits off from the $k = 4$ branch when $H > 0$. The colored dots correspond to solutions that are examined in more detail below. Unlike the Whitham $(T = 0)$ case, the diagram shows that as the speed of the solution decreases, the wave height increases. Ehrnström Wahlén [26] proved that, in the small-amplitude limit, the relationship between wave height and speed is determined by the ratio of the wave number and period of the solution.

Figure 7(a) includes plots of four different $k = 2$ (i.e. period π), traveling-wave solutions to the cW equation with $T = 0.2$. Unlike solutions of the Whitham equation which are waves of elevation, these solutions are waves of depression. As the wave height increases, the solution speed decreases. Although the bifurcation diagram suggests that a maximal wave height does not exist, we were not able to prove it, numerically or otherwise. As wave speed decreases, the solutions become steeper waves of depression with increasing wave height. This is consistent with the Ehrnström *et al.* [22] result that the solutions limit to a constant solution in the L^2, but not L^∞, sense. However, note that Ehrnström *et al.* [22] proved that all periodic, traveling-wave solutions to the cW equation are smooth. Figure 7(b) contains plots of the corresponding linear stability spectra. All four of these solutions are unstable. Just as with solutions to the Whitham equation, the maximal instability growth rate of these solutions increases as their wave heights

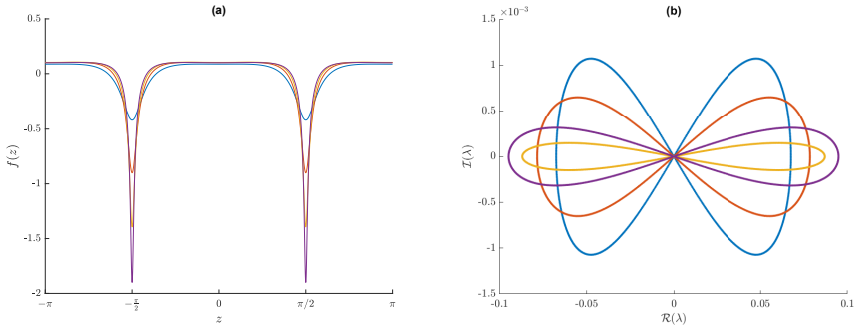

Figure 7. Plots of (a) four representative solutions of the cW equation with $T = 0.2$ and $k = 2$ and (b) their stability spectra. The wave speeds and heights of these solutions are $c = 0.7609$ and $H = 0.5060$ (blue), $c = 0.5369$ and $H = 1.004$ (orange), $c = 0.3289$ and $H = 1.499$ (yellow), and $c = 0.1369$ and $H = 2.002$ (purple).

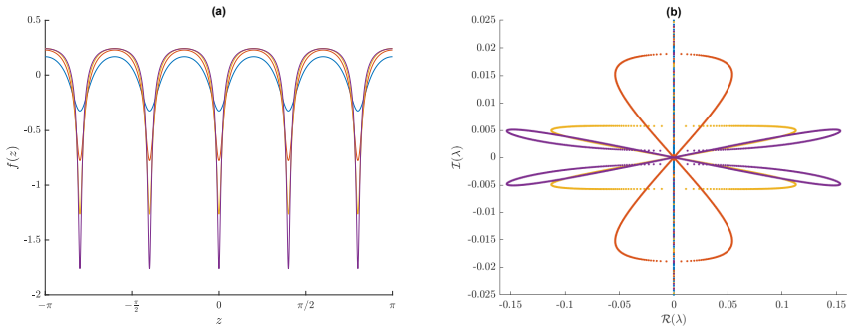

Figure 8. Plots of (a) four representative solutions of the cW equation with $T = 0.2$ and $k = 5$ and (b) their stability spectra. The wave speeds and heights of these solutions are $c = 1.016$ and $H = 0.4972$ (blue), $c = 0.8364$ and $H = 1.005$ (orange), $c = 0.6334$ and $H = 1.508$ (yellow), and $c = 0.4374$ and $H = 2.002$ (purple).

increase. Additional numerical simulations (not shown) establish that all small-amplitude, traveling-wave solutions with $k = 2$ and $T = 0.2$ are unstable.

Figure 8(a) includes plots of four $k = 5$, traveling-wave solutions to the cW equation with $T = 0.2$. Figure 7(b) shows the corresponding stability spectra. These four solutions have approximately the same wave heights as the four $k = 2$ solutions shown in Figure 7(a). Other than their period and speeds, the $k = 5$ solutions are qualitatively similar to the $k = 2$ solutions. The solution with the smallest wave height (blue) is spectrally stable. This is qualitatively different than what happens in the $T = 0$ case where all small-amplitude solutions with $k > 1.145$ are unstable. The three solutions with larger wave height are unstable and the maximal instability growth rate increases with wave height. Additional numerical simulations (not shown) establish that solutions with $k \in (2, 5)$ have similar properties to the solutions presented in Figures 7-8. There exists a $k^\dagger \in (2, 5)$ where the small-amplitude solutions switch from being unstable to spectrally stable.

Figure 9 contains plots of four representative solutions from the bifurcation branch that splits off from the $k = 4$ branch. These solutions are qualitatively different than the solutions examined above, but have approximately the same wave heights as the solutions shown in Figures 7(a) and 8(a). These solutions are similar to the mixed-mode solutions examined by Remonato & Kalisch [23]. For solutions with crests of multiple heights, we define wave height to be the maximum value of the solution minus the minimum value of the solution. Figure 9(b), shows that the stability spectra are also qualitatively different

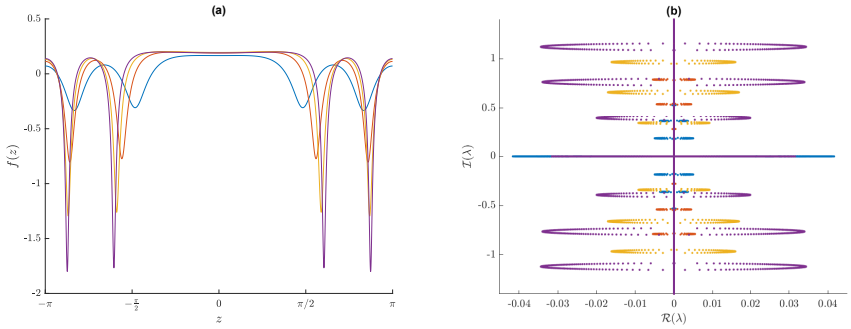

Figure 9. Plots of (a) four representative solutions of the cW equation with $T = 0.2$ from the solution branch that does not touch the horizontal axis in Figure 6 and (b) their stability spectra. The wave speeds and heights of these solutions are $c = 0.9540$ and $H = 0.5008$ (blue), $c = 0.7614$ and $H = 1.002$ (orange), $c = 0.5563$ and $H = 1.498$ (yellow), and $c = 0.3574$ and $H = 1.999$ (purple).

than those examined above. The spectra for each solution includes a horizontal figure 8 centered at the origin. (In the figure, these figure 8s appear as horizontal lines along $\mathcal{I}(\lambda) = 0$ due to scaling.) Thus, each solution is unstable with respect to the modulational instability. Each spectrum has six additional "bubbles" centered on the $\mathcal{I}(\lambda)$ axis. (Only four of the blue bubbles are easily visible due to scaling.) The solution with smallest wave height (the blue solution) has the largest maximum instability growth rate. But, there does not appear to be a simple relationship between wave height and the maximum instability growth rate in this case.

3.2.2. Surface tension parameter $T = \frac{1}{3}$

Figure 10 includes a portion of the bifurcation diagram for $T = \frac{1}{3}$. The colored dots correspond to solutions that are examined in more detail below. These solutions have approximately the same wave heights as the colored solutions examined in other sections. The bifurcation diagram shows that as wave speed decreases, wave height increases for all branches (that we examined). This is consistent with the Ehrnström *et al.* [22] result that the solutions limit to a constant solution in the L^2, but not L^∞, sense.

Figures 11 and 12 include plots of $k = 1$ and $k = 2$ solutions and their stability spectra for $T = \frac{1}{3}$. All eight of these solutions are unstable and their spectra are shaped like horizontal figure 8s. As wave height increases, the maximal instability growth rate also increases. The $k = 2$ solutions have larger instability growth rates than the $k = 1$ solutions with the same wave height.

Figures 13 includes plots of the $k = 5$ solutions and their stability spectra for $T = \frac{1}{3}$. Other than their periods, these solutions appear to be qualitatively similar to the $k = 1$ and $k = 2$ solutions. However, their stability spectra lie completely on the $\mathcal{I}(\lambda)$ axis. This means that all four of these solutions,regardless of their wave height, are spectrally stable. This numerically establishes that when $T = \frac{1}{3}$ there are some intervals of k space in which the small-amplitude, periodic, traveling-wave solutions are spectrally stable and other regions of k space in which these solutions are unstable.

3.2.3. Surface tension parameter $T = 0.4$

Figure 14 includes a portion of the bifurcation diagram for $T = 0.4$. The colored dots correspond to solutions that are examined in more detail below. These solutions have approximately the same wave heights as the colored solutions examined in other sections. The bifurcation diagram shows that as wave speed decreases, wave height increases for all branches (that we examined).

Figure 15 includes plots of four representative $k = 1$ solutions to the cW equation with $T = 0.4$ and their stability spectra. All four of these solutions are unstable and the growth rate of the instabilities

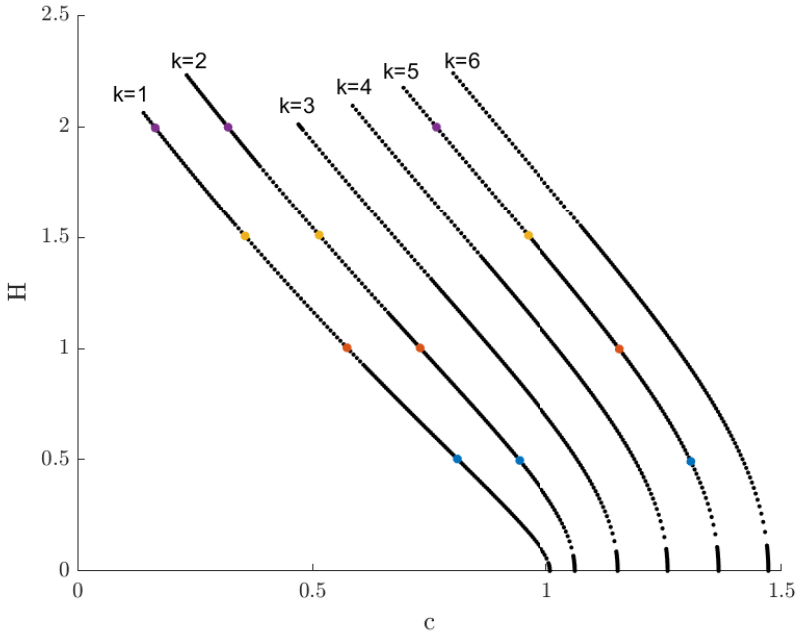

Figure 10. A portion of the bifurcation diagram for the capillary Whitham equation with $T = \frac{1}{3}$. The colored dots correspond to solutions that are examined in more detail in Figures 11-13.

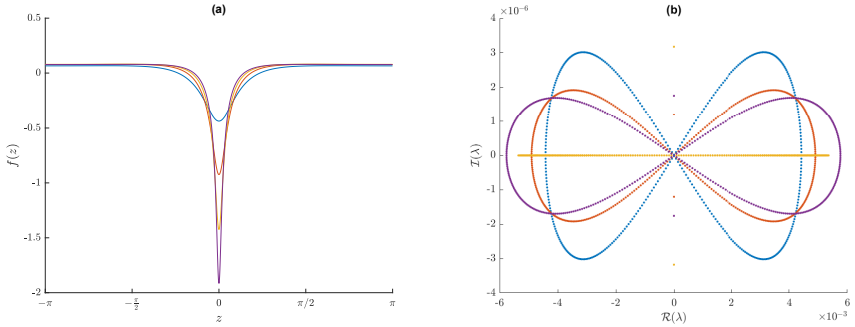

Figure 11. Plots of (a) four representative solutions of the cW equation with $T = \frac{1}{3}$ and $k = 1$ and (b) their stability spectra. The wave speeds and heights of these solutions are $c = 0.8087$ and $H = 0.5036$ (blue), $c = 0.5737$ and $H = 1.003$ (orange), $c = 0.3567$ and $H = 1.506$ (yellow), and $c = 0.1657$ and $H = 1.994$ (purple).

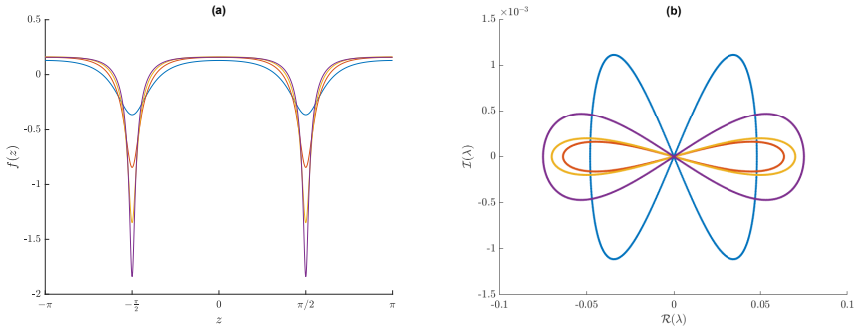

Figure 12. Plots of (a) four representative solutions of the cW equation with $T = \frac{1}{3}$ and $k = 2$ and (b) their stability spectra. The wave speeds and heights of these solutions are $c = 0.9415$ and $H = 0.4970$ (blue), $c = 0.7295$ and $H = 1.002$ (orange), $c = 0.5145$ and $H = 1.509$ (yellow), and $c = 0.3205$ and $H = 1.997$ (purple).

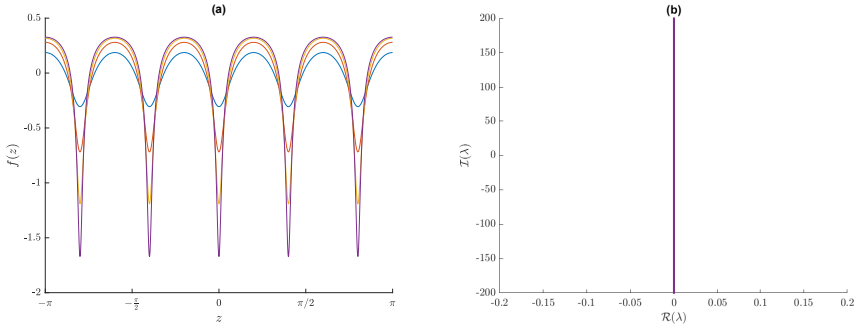

Figure 13. Plots of (a) four representative solutions of the cW equation with $T = \frac{1}{3}$ and $k = 5$ and (b) their stability spectra. The wave speeds and heights of these solutions are $c = 1.307$ and $H = 0.4924$ (blue), $c = 1.155$ and $H = 0.9975$ (orange), $c = 0.9602$ and $H = 1.508$ (yellow), and $c = 0.7642$ and $H = 1.998$ (purple).

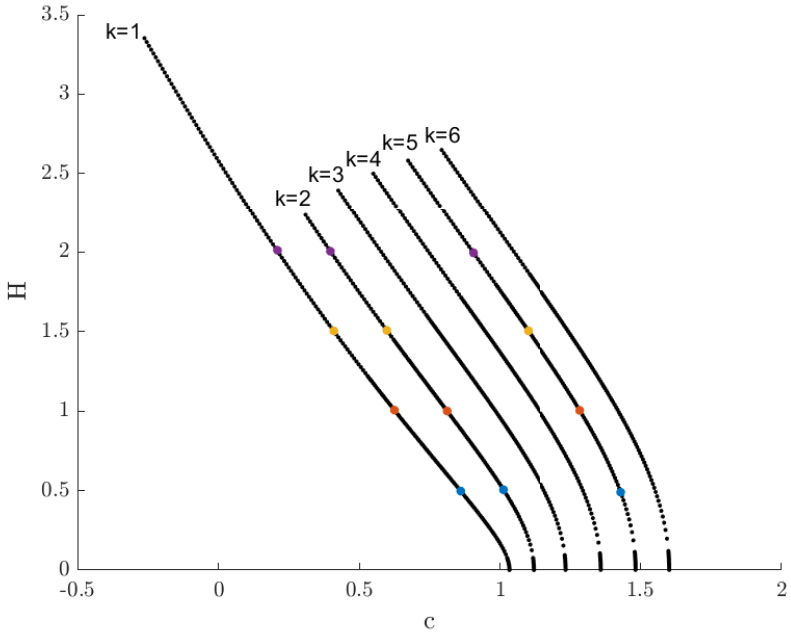

Figure 14. A portion of the bifurcation diagram for the cW equation with $T = 0.4$. The colored dots correspond to solutions that are examined in more detail in Figures 15-17.

increases as the wave height of the solution increases. Figure 16 shows that all four $k = 2$ solutions are spectrally stable while Figure 17 shows that all four $k = 5$ solutions are unstable. This numerically establishes that when $T = 0.4$ there are some intervals of k space in which the small-amplitude, periodic, traveling-wave solutions are spectrally stable and other regions of k space in which these solutions are unstable.

3.2.4. Surface tension parameter $T \approx 0.1582$

Remonato & Kalisch [23] presented the following formula which allows T values to be chosen so that solutions corresponding to any two k values will have the same wave speed in the small-amplitude limit

$$T = T(k_1, k_2) = \frac{k_1 \tanh(k_2) - k_2 \tanh(k_1)}{k_1 k_2 (k_1 \tanh(k_1) - k_2 \tanh(k_2))}. \tag{14}$$

Using this formula with $k_1 = 1$ and $k_2 = 4$ gives $T \approx 0.1582$, which is the final T value we examine. A portion of the corresponding bifurcation diagram is included in Figure 18. The fact that the $k = 1$ and $k = 4$ solutions have the same speed in the small-amplitude limit is exemplified by the fact that there are two branches leaving the same point on the c axis near $c = 0.94$. These branches correspond to the $k = 4$ solution and a $k = (1, 4)$ branch. Here, the notation $k = (a, b)$ means that the solution is composed of a linear combination of the $k = a$ and $k = b$ wavenumbers in the small-amplitude limit. We were unable to isolate the $k = 1$ solution. We note that Remonato & Kalisch [23] made a similar observation for their $(1, 7)$ solution.

Figure 19 shows that solutions on the $k = 4$ branch with small wave height are spectrally stable, while those with large wave height are unstable. These solutions do not have the striking increasingly steep wave of depression form that the cW solutions presented above have. As wave height increases, the growth rates of the instabilities also increase.

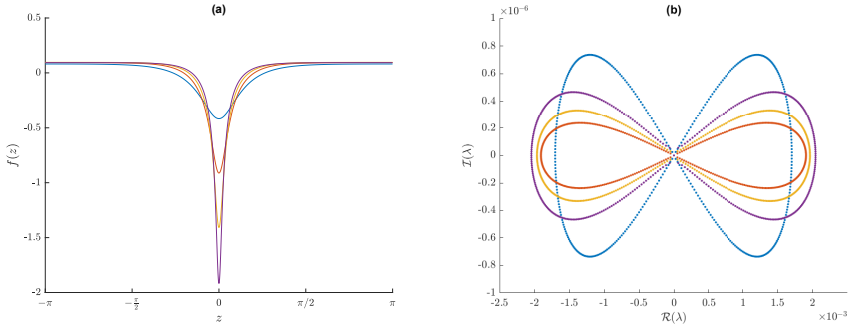

Figure 15. Plots of (a) four representative solutions of the cW equation with $T = 0.4$ and $k = 1$ and (b) their stability spectra. The wave speeds and heights of these solutions are $c = 0.8596$ and $H = 0.4969$ (blue), $c = 0.6246$ and $H = 1.006$ (orange), $c = 0.4096$ and $H = 1.504$ (yellow), and $c = 0.2096$ and $H = 2.011$ (purple).

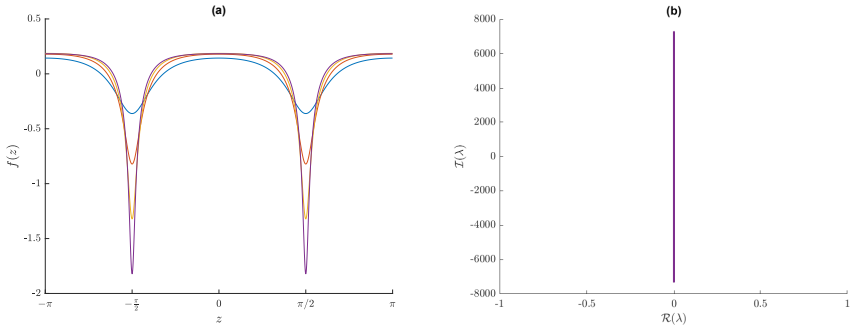

Figure 16. Plots of (a) four representative solutions of the cW equation with $T = 0.4$ and $k = 2$ and (b) their stability spectra. The wave speeds and heights of these solutions are $c = 1.012$ and $H = 0.5051$ (blue), $c = 0.8115$ and $H = 1.000$ (orange), $c = 0.5975$ and $H = 1.507$ (yellow), and $c = 0.3975$ and $H = 2.005$ (purple).

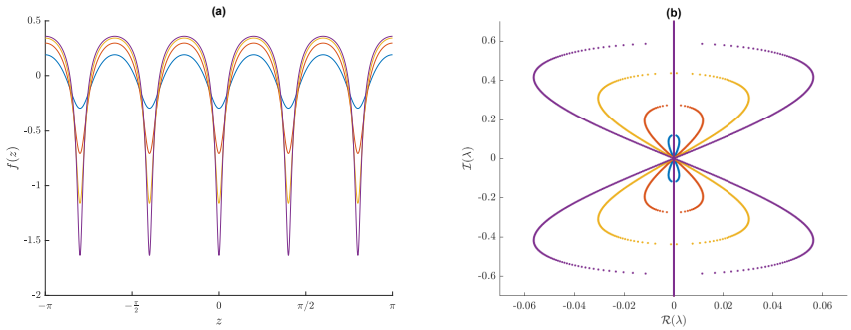

Figure 17. Plots of (a) four representative solutions of the cW equation with $T = 0.4$ and $k = 5$ and (b) their stability spectra. The wave speeds and heights of these solutions are $c = 1.430$ and $H = 0.4897$ (blue), $c = 1.285$ and $H = 1.004$ (orange), $c = 1.100$ and $H = 1.504$ (yellow), and $c = 0.9052$ and $H = 1.995$ (purple).

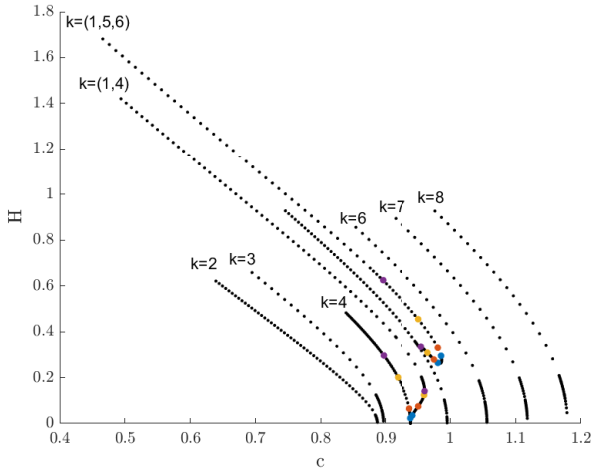

Figure 18. A portion of the bifurcation diagram for the cW equation with $T \approx 0.1582$. The colored dots correspond to solutions that are examined in more detail in Figures 19-22.

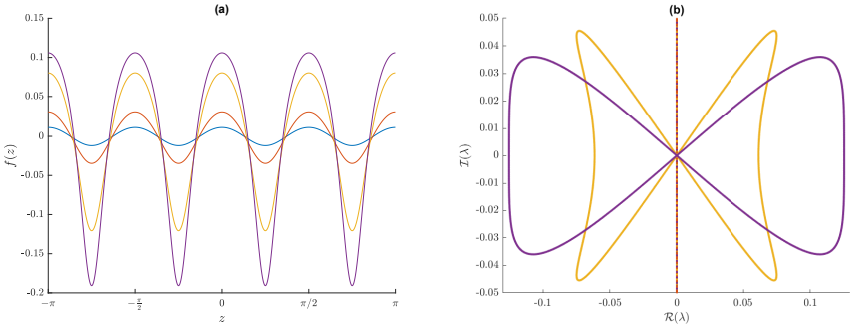

Figure 19. Plots of (a) four representative solutions of the cW equation with $T \approx 0.1582$ and $k = 4$ and (b) their stability spectra.

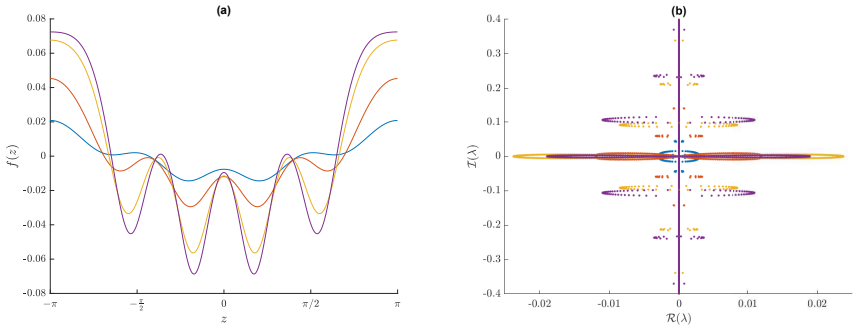

Figure 20. Plots of (a) four representative solutions of the cW equation with $T \approx 0.1582$ and $k = (1,4)$ and (b) their stability spectra.

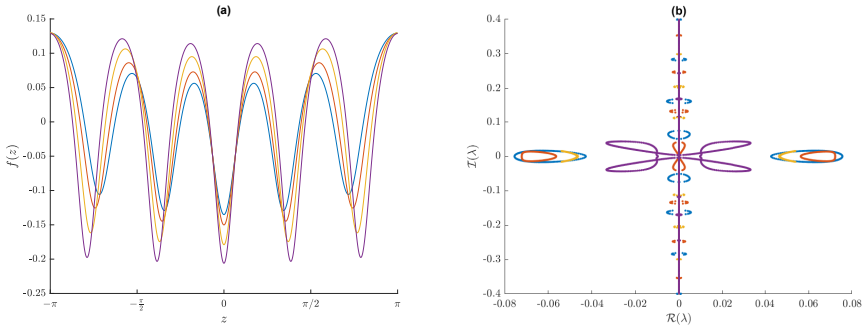

Figure 21. Plots of (a) four representative solutions of the cW equation with $T \approx 0.1582$ and $k = (1,5)$ and (b) their stability spectra.

Figure 20 includes plots of four representative $k = (1,4)$ solutions and their stability spectra. These solutions do not have the increasingly steep wave of depression form of the majority of the other cW solutions. The spectra of these $k = (1,4)$ solutions are similar to those in Figure 9(b). This is likely due to the fact that both of these sets of solutions have more than one dominant Fourier mode. Each spectrum has a horizontal figure 8 centered at the origin and six bubbles centered on the $\mathcal{I}(\lambda)$ axis. The solution with the largest wave height is not the most unstable solution.

Figure 18 shows that there is a secondary branch that splits off from the $k = 5$ branch at $H \approx 0.39$. As expected, the solutions along this branch do not have a single dominant wavenumber. The solutions on this branch are $k = (1,5)$ solutions until the branch curves around and heads upward. The solutions after this turning point are $k = (1,5,6)$ solutions. Figure 21(a) includes plots of four $k = (1,5)$ solutions and their stability spectra. All four of these solutions are unstable and have complicated spectra. Figure 22 includes plots of four representative $k = (1,5,6)$ solutions and shows that they are unstable. All four solutions have horizontal figure 8s centered at the origin and four bubbles centered along the $\mathcal{I}(\lambda)$ axis. The solution with smallest wave height is the most unstable.

4. Summary

Bottman & Deconinck [27] proved that all traveling-wave solutions of the KdV equation are stable. This is quite different than the Whitham equation where all large-amplitude solutions are unstable [9] and only small-amplitude solutions with a wavenumber $k > 1.145$ are stable [8,9].

We began by examining large-amplitude, 2π-periodic, traveling-wave solutions to the Whitham equation (with zero surface tension). We found that all such solutions are unstable and that their stability

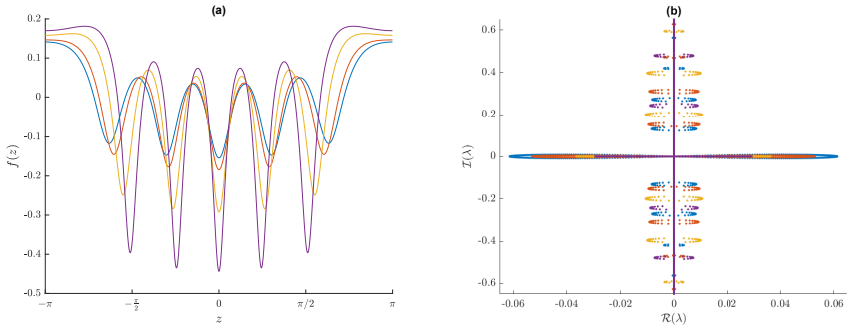

Figure 22. Plots of (a) four representative solutions of the cW equation with $T \approx 0.1582$ and $k = (1, 5, 6)$ and (b) their stability spectra.

T \ k	1	2	3	4	5
0	su	uu	uu	uu	uu
0.1582...		uu	uu	su	su
0.2		uu	uu	uu	su
1/3	uu	uu	ss	ss	ss
0.4	uu	ss	ss	ss	uu

Table 1. A summary of stability results for single-mode, periodic, traveling-wave solutions with period 2π, wavenumber k, and surface tension parameter T. The first letter in each cell signifies if small-amplitude solutions are spectrally stable (s) or unstable (u). The second letter in each cell signifies if moderate- and large-amplitude solutions are spectrally stable or unstable. We were unable to compute the solutions corresponding to the cells that are left blank.

spectra undergo two bifurcations as wave height increases. We also found that the instability growth rate increases with wave height.

Next, we examined periodic, traveling-wave solutions to the capillary-Whitham equation with four different nonzero values of the surface tension parameter, T. We found that the cW solutions and their stability were more diverse than in the Whitham ($T = 0$) case. Most of the solutions we examined were waves of depression. In contrast, all periodic, traveling-wave solutions to the Whitham equation are waves of elevation. We found that as wave height increases, wave speed decreases (and can become negative). We were not able to determine if the cW equation admits a solution with maximal wave height. In contrast, the Whitham equation has a solution with maximal wave height. We computed periodic, traveling-wave solutions with for a wide range of wavenumbers, but were not able to compute solutions of all wavenumbers for all values of T. In addition to computing a variety of solutions with a single dominant wavenumber, we computed four families of solutions that had multiple dominant wavenumbers.

We examined the stability of all of the cW solutions we computed. Table 1 contains a summary of our results. We found that some solutions were spectrally stable and others were unstable. There are regions of (k, T)-space where small-amplitude, periodic, traveling-wave solutions are spectrally stable and large-amplitude solutions are unstable. There appear to be other regions of (k, T)-space where all solutions, regardless of amplitude, are spectrally stable. The exact topology of these regions remains an open question. If the solutions had a single dominant wavenumber, then the maximal instability growth rate increased with wave height. If the solutions had multiple dominant wavenumbers, there was not a simple relationship between instability growth rates and wave heights. Finally, we found some solutions for which the modulational instability was the dominant instability and other solutions that had other

dominant instabilities. However, all unstable solutions we examined were unstable with respect to the modulational instability.

We thank Mats Ehrnström, Vera Hur, Mat Johnson, Logan Knapp, and Olga Trichtchenko for helpful discussions. This material is based upon work supported by the National Science Foundation under grant DMS-1716120.

1. Trillo, S.; Klein, M.; Clauss, G.; Onorato, M. Observation of dispersive shock waves developing from initial depressions in shallow water. *Physica D* **2016**, *333*, 276–284.
2. Carter, J. Bidirectional Whitham equations as models of waves on shallow water. *Wave Motion* **2018**, *82*, 51–61.
3. Whitham, G. Variational methods and applications to water waves. *Proceedings of the Royal Society of London, A* **1967**, *299*, 6–25.
4. Whitham, G. *Linear and Nonlinear Waves*; John Wiley & Sons, Inc., New York, 1974.
5. Ehrnström, M.; Kalisch, H. Traveling waves for the Whitham equation. *Differential and Integral Equations* **2009**, *22*, 1193–1210.
6. Ehrnström, M.; Groves, M.; Wahlén, E. On the existence and stability of solitary-wave solutions to a class of evolution equations of Whitham type. *Nonlinearity* **2012**, *25*, 2903–2936.
7. Arnesen, M. Existence of solitary-wave solutions to nonlocal equations. *Discrete and Continuous Dynamical Systems. Series A* **2016**, *36*, 3483–3510.
8. Johnson, M.; Hur, V. Modulational instability in the Whitham equation for water waves. *Studies in Applied Mathematics* **2015**, *134*, 120–143.
9. Sanford, N.; Kodama, K.; Carter, J.; Kalisch, H. Stability of traveling wave solutions to the Whitham equation. *Physics Letters A* **2014**, *378*, 2100–2107.
10. Kalisch, H.; Moldabayev, D.; Verdier, O. A numerical study of nonlinear dispersive wave models with SpecTraVVave. *Electronic Journal of Differential Equations* **2017**, *62*, 1–23.
11. Moldabayev, D.; Kalisch, H.; Dutykh, D. The Whitham equation as a model for surface water waves. *Physica D* **2015**, *309*, 99–107.
12. Klein, C.; Linares, F.; Pilod, D.; Saut, J.C. On Whitham and related equations. *Studies in Applied Mathematics* **2017**, *140*, 133–177.
13. Deconinck, B.; Trichtchenko, O. High-frequency instabilities of small-amplitude Hamiltonian PDEs. *Discrete and Continuous Dynamical Systems* **2015**, *37*, 1323–1358.
14. Dinvay, E.; Moldabayev, D.; Dutykh, D.; Kalisch, H. The Whitham equation with surface tension. *Nonlinear Dynamics* **2017**, *88*, 1125–1138.
15. Vanden-Broeck, J.M. *Gravity-Capillary Free-Surface Flows*; Cambridge University Press, 2010.
16. Crapper, G. An exact solution for progressive capillary waves of arbitrary amplitude. *Journal of Fluid Mechanics* **1957**, *2*, 532–540.
17. Trulsen, K.; Kliakhandler, I.; Dysthe, K.; Verlarde, M. On weakly nonlinear modulation of waves on deep water. *Phyiscs of Fluids* **2000**, *12*, 2432.
18. Sulem, C.; Sulem, P.L. *The Nonlinear Schrödinger Equation: Self-Focusing and Wave Collapse*; Springer, 1999.
19. Akers, B.; Ambrose, D.; Wright, J. Gravity perturbed Crapper waves. *Proceedings of the Royal Society A* **2014**, *470*, 20130526.
20. Akers, B.; Milewski, P. Model equations for gravity-capillary waves in deep water. *Studies in Applied Mathematics* **2008**, *121*, 49–69.
21. Akers, B.; Milewski, P. A model equation for wavepacket solitary waves arizing from graity-capillary flows. *Studies in Applied Mathematics* **2009**, *122*, 249–274.
22. Ehrnström, M.; Johnson, M.; Maehlen, O.; Remonat, F. On the bifurcation diagram of the capillary-gravity Whitham equation. *arXiv:1901.03534 [math.AP]* **2019**.
23. Remonato, F.; Kalisch, H. Numerical bifurcation for the capillary Whitham equation. *Physica D* **2017**, *343*, 51–62.

24. Hur, V.; Pandey, A. Modulational instability in a full-dispersion shallow water model. *Studies in Applied Mathematics* **2019**, *142*, 3–47.
25. Deconinck, B.; Kutz, J. Computing spectra of linear operators using Hill's method. *Journal of Computational Physics* **2006**, *219*, 296–321.
26. Ehrnström, M.; Wahlén, E. On Whitham's conjecture of a highest cusped wave for a nonlocal shallow water wave equation. *Annales de l'Institut Henri Poincaré C, Analyse non linéaire* **2019**, p. In press.
27. Bottman, N.; Deconinck, B. KdV cnoidal waves are linearly stable. *Discrete and Continuous Dynamical Systems A* **2009**, *25*, 1163–1180.